University of Birmingham
Research at Birmingham

Optical scattering from graphene foam for oil imaging/sensing

Deng, Sunan; Kidambi, Piran R.; Butt, Haider; Sabouri, Aydin; Sohail, Manzar; Khan, Safyan A.; Jiang, Kyle

DOI:
10.1039/c6ra15134e

License:
None: All rights reserved

Document Version
Peer reviewed version

Citation for published version (Harvard):
Deng, S, Kidambi, PR, Butt, H, Sabouri, A, Sohail, M, Khan, SA & Jiang, K 2016, 'Optical scattering from graphene foam for oil imaging/sensing', *RSC Advances*, vol. 6, no. 76, pp. 71867-71874.
https://doi.org/10.1039/c6ra15134e

Link to publication on Research at Birmingham portal

General rights
Unless a licence is specified above, all rights (including copyright and moral rights) in this document are retained by the authors and/or the copyright holders. The express permission of the copyright holder must be obtained for any use of this material other than for purposes permitted by law.

•Users may freely distribute the URL that is used to identify this publication.
•Users may download and/or print one copy of the publication from the University of Birmingham research portal for the purpose of private study or non-commercial research.
•User may use extracts from the document in line with the concept of 'fair dealing' under the Copyright, Designs and Patents Act 1988 (?)
•Users may not further distribute the material nor use it for the purposes of commercial gain.

Where a licence is displayed above, please note the terms and conditions of the licence govern your use of this document.

When citing, please reference the published version.

Take down policy
While the University of Birmingham exercises care and attention in making items available there are rare occasions when an item has been uploaded in error or has been deemed to be commercially or otherwise sensitive.

If you believe that this is the case for this document, please contact UBIRA@lists.bham.ac.uk providing details and we will remove access to the work immediately and investigate.

Download date: 25. Apr. 2024

WILEY-VCH

DOI: 10.1002/ ((please add manuscript number))

Article type: Full Paper

Optical scattering from graphene foam for oil imaging/sensing

Sunan Deng, Piran R. Kidambi, Haider Butt, Aydin Sabouri, Manzar Sohail, Safyan A. Khan, Kyle Jiang,*

S. Deng, Dr.A.Sabouri , Prof. K. Jiang. Dr. H.Butt
School of Mechanical Engineering, University of Birmingham, Birmingham B15 2TT, UK
E-mail: H.Butt@bham.ac.uk
Dr. P.R.Kidambi
Department of Mechanical Engineering, Massachusetts Institute of Technology, Cambridge, MA, USA

Dr. M. Sohail, Dr. S. A. Khan,

Center of Excellence in NanoTechnology, King Fahd University of Petroleum and Minerals, Dhahran 31261, Saudi Arabia

Keywords: Graphene foam, oil sensor, diffraction, optical scattering

ABSTRACT: Oil spill detection is crucial, both from an environmental perspective and the associated economic losses. Current optical oil sensing techniques, such as underwater microscopy and light scattering methods, mainly focus on detecting the properties of particles or organisms in water and often require costly equipment and sophisticated data processing. Recent studies on graphitic foam show its extraordinary pollutant absorbing properties, with high absorption weight ratios. Here we propose to produce a graphene foam based ultra-light material that changes its optical properties on absorbing oil species. The results demonstrate clear changes in

optical transmission and scattering properties of graphene foam when exposed to various oils. The effective graphene foam sorbent can be easily integrated with optic fibers systems to detect the optical property variations and also to monitor oil presence/spillages remotely. Such sensors can also be used for underground oil exploration.

1.Introduction

The leakage of oil leads to a disastrous consequences in various industries, resulting in massive economical losses and, more importantly environmental pollution. Developing oil sensor to diagnose the oil leak at early stage before they causing widespread damage is crucial.[1] Petroleum hydrocarbons (HC) present a multiphase mix consisting of liquid, dissolved gaseous or solid phase in seawater.[2] Direct oil sensors detect methane, polyaromatic hydrocarbons, or hydrocarbons (HC) in seawater directly, while indirect oil sensors rely on discriminating the properties of the local seawater environment with and without the presence of oil. The indirect methods mainly include measurement of seawater physical properties (such as concentration of oxygen or CO_2), optical light scattering, and under water microscopy. Optical light scattering method [3, 4] is usually used to detect the scattered light or diffraction patterns of the suspended and undissolved materials in a water sample, while underwater microscopy [5-7] is used for analysing microscopic organism to support dispersant injection,[8-10] which reduce the oil to small droplets and increase microbial degeneration.[11, 12] The existing optical methods, which focus on detecting the particles or organisms in the water generally require highly sensitive/expensive sensors to identify the small sized particles and also suffer from time consuming and complicate data processing.

Graphene foam (GF), taking advantages of its ultra-light weight,[13] high surface area and porous structure, has been recently proposed as a versatile and recyclable sorbent material. It shows highly efficient absorption of petroleum products and fats (up to 86 times of its own weight), requiring no further pretreatment, which is tens of times higher than that of conventional absorbers.[14-17] Additionally, *via* simple heat treatment, the graphene foam can be reused up to 10 times without a drop in performance.[14, 15] Hence, the graphene foam can have widespread potential applications in environmental protection as well as in oil exploration.

In this paper we present a novel study on the optical transmission and scattering properties of graphene foam. Clear changes in these optical effects that occur due to the absorption of various oil species were observed. The presence of oil droplets in graphene foam leads to much stronger scattering effects, a change that can be easily detected remotely via optic fibres and imaging systems. Imaging of oil soaked graphene foam in multiple optical microscope detection modes demonstrates the presence of oil droplets (causing scattering) and also aid in their identification. Therefore, with the graphene foam, the efficiency of current underwater microscope and scattering based oil spill detection methods can be enhanced.

2.Fabrication of graphene foam

The graphene foam samples were fabricated by chemical vapour deposition (CVD) method via nickel foam template, with pore size about 450 µm, area density 420 g/m^2 and total thickness of 1.6 mm**.**[18] After the CVD process, the few layer graphene (FLG) covered Ni scaffold was trimmed along the edges to create access for $FeCl_3$ solution, which etched the nickel to produce the free-standing FLG foam. Then the sample was washed by deionised (DI) water and etched in 10% HCl to remove Fe. Finally, after being washed again in DI water and rinsed in iso-propanol (IPA), the graphene foam was dried in ambient air. Figure 1(a) and (b) show the optical and SEM images of graphene foam, where the multi-layer network structure can be observed.

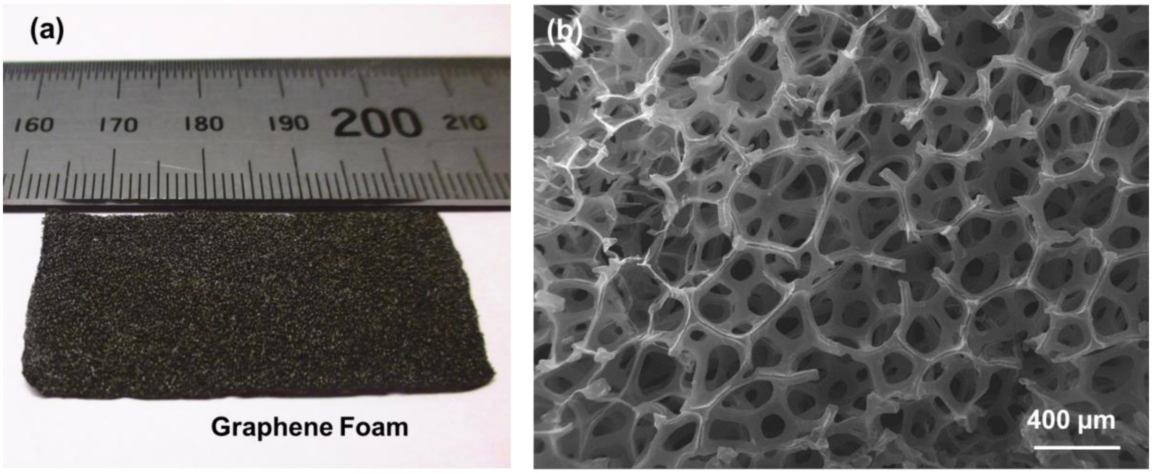

Figure 1. (a) Optical images of graphene foam. (b) SEM image of graphene foam.

3. Transmission studies on graphene foam/oils composite samples.

The transmission spectra for graphene foam and the three oils are shown in Figure 2(a). It can be seen that compared with glass (reference), the transmission of nickel and graphene foam are very low (less than 8%). Because of the similar structure, the transmission curves of the two foams are similar in shapes. The transmittances for various oil species (used in our study: stroke, supercut and turbo oils) were also measured, Figure 2(b). The solid lines are transmission spectra for oils in plastic container with oil depths of about 2 mm. Empty containers were used as reference. As for the dash lines, these are transmission spectra for oils in graphene foam with reference to empty foams. The measurements were done under oil saturate conditions and it was found that the transmission through the foams was sensitive even for 0.5 µL oil, before saturation points. By combing with optical fibre sensing, it will be possible to detect minute amounts of oil and construct an GF based oil sensor.

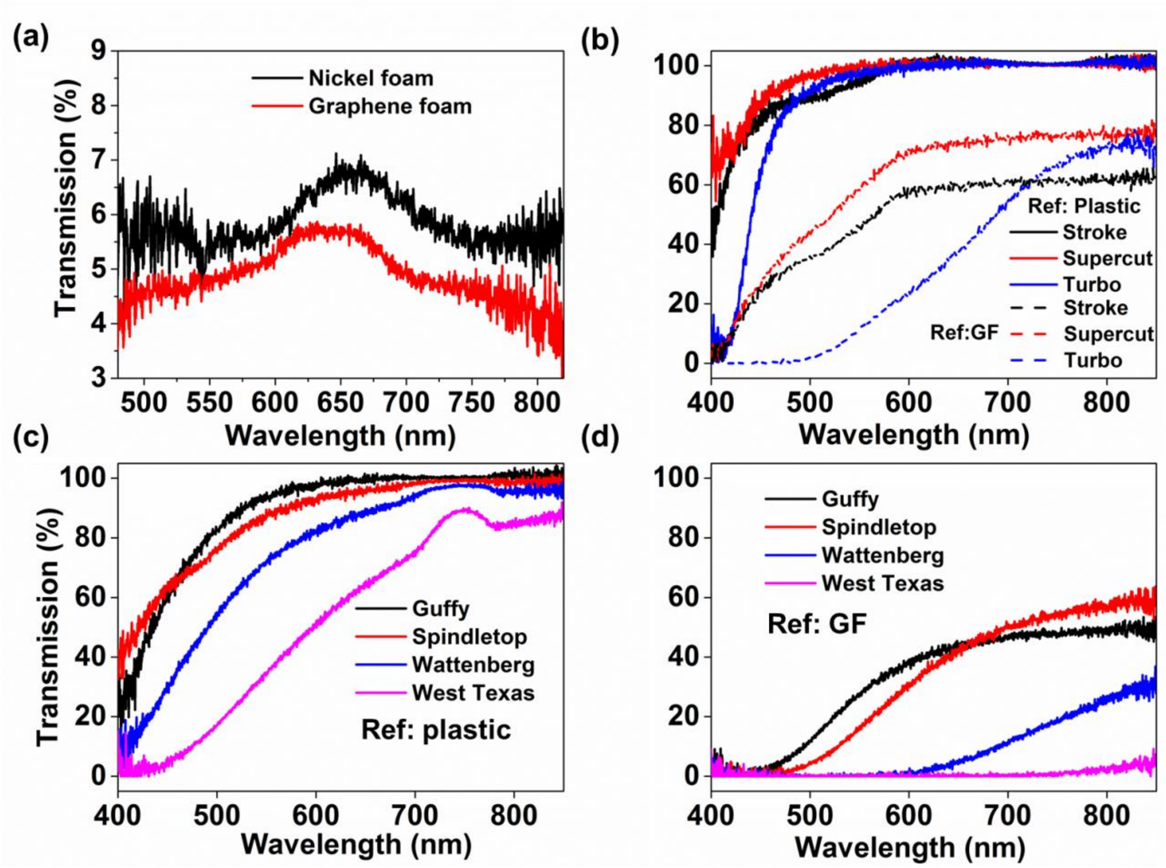

Figure 2. (a) Transmissions of graphene and Nickel foam, with reference to glass slide. The thickness for both of the foams was near 1.6 mm. (b) Transmissions of stroke oil, supercut oil, and turbo oil (solid lines) with respect to standard plastic container. Dashed lines refer to the oils soaked in GF, with empty GF as reference. (c) Transmission spectra for crude oils (including oils from Guffy, Spindletop, Wattenberg, and West Texas refineries). (d) Transmission spectra for crude oils when soaked in GF. The depth of oils in plastic container was about 2 mm.

In wavelength ranges from 400 to 500 nm, all of the oils in plastic container have very low transmissions, which relate to high absorption, especially for the turbo oil, with a near zero transmission at 400 nm. The different absorptions in short wavelength regime (<550 nm) result in the difference of visual colours of the three oils, as they have almost the same transmissions, about 100%, in longer wavelengths (>600 nm).

For wavelengths at 400-600 nm, the transmission of stroke oil in graphene foam is very similar to that in plastic container, with the same characteristic shape but different intensity. The supercut oil still has a higher transmission in GF than the other two oils, just as it does in plastic. The shape of transmission for turbo oil in graphene foam is very different from that in plastic, and this may due to the scattering effects.

Thus detection of oils transmission signatures can be an efficient way for differentiating the oil species. Most oils have characteristic transmission curves, although the transmission spectrum may change in the graphene foam due to the scattering effect. However, the species can be identified by comparing with transmission in transparent container. For example, it can be employed to achieve the identical characteristic behaviour, or considered by the relative relationships between different oils.

Four kinds of crude oils (sourced from Wattenberg, Spindletop, West Texas, and Guffey oil fields) in graphene foam were also studied, as illustrated in Figure 2(c-d). In order to investigate the optical properties of crude oils in graphene foam, the transmissions measurements were performed. As shown in Fig 2(c), a low transmission efficiency in short wavelength regime (< 500 nm) indicated strong corresponding absorption. Although with different colours in bottles, transmission of Spindletop oil is very close to Guffy oil, but with larger absorption in the range 470 -

700 nm. The transmissions of West Texas and Wattenberg oils were much lower than the other two oils in the whole visible regime.

Figure 2(d) shows transmission spectra for crude oils in GF, with GF without oil as a reference. Negligible transmission (due to strong absorption) takes places through GF containing West Texas and Wattenberg oils for light with wavelength shorter than 600 nm. Transmission for Wattenberg oil increase gradually up to 30% for larger wavelengths, while that for West Texas remains near zero. As for Spindletop oil, its transmission is higher than that of Guffy oil for red light with wavelength longer than 650 nm, but has a lower transmittance for green and yellow light. It can also be noticed that the blue light with wavelengths smaller 470 nm is absorbed by all the crude oil samples tested.

4.Graphitic foam for oil spill detection based on optical imaging method.

Optical imaging measurements of graphene foam with and without oil were performed to explore the possibility of using graphene foam to detect oil environments. This study also sheds light on the optical properties and various scattering effects displayed by the graphene foam plus oils composites. A Carl Zeiss Scope A1 optical microscope was used which was equipped with several detection modes (dark and bright field). The microscope can be operated under reflected or transmitted light or with a combination of both. As for reflected (R) mode of incident light, both the bright field (BF) and dark field (DF) mode were studied, while for transmitted (T) light, bright field and phase contrast modes were studied. The phase contrast method transfers the phase-shift into intensity or colour difference and has three phase modes (Ph 1- 3) with varying numeral apertures adjusted by different ring diaphragms. Relevant modes of the microscope are further discussed in supporting information (Figure S1) with images of graphene/oil composites in various modes.

Figure 3 demonstrates optical images of graphene foam with and without oil in various optical modes. Various oil species were studied analysed (supporting information S2-S5) but due to the most clarity the results for GF soaked with stroke oil are presented in Fig 3 (d-f) under three detection modes. All the optical imaging was performed at the same position in GF while illuminating with constant intensity of both reflected/transmitted light simultaneously, with identical objectives and detection modes. Figure 3 (a-b) only show the GF in various optical modes. In the dark field (DF) modes the microscope blocks the normally propagating unperturbed light rays and only allows the scattered light waves through the objectives, hence the darker images. This allows the viewing of sharp edges and objects which are of the same scale as the wavelengths of light.

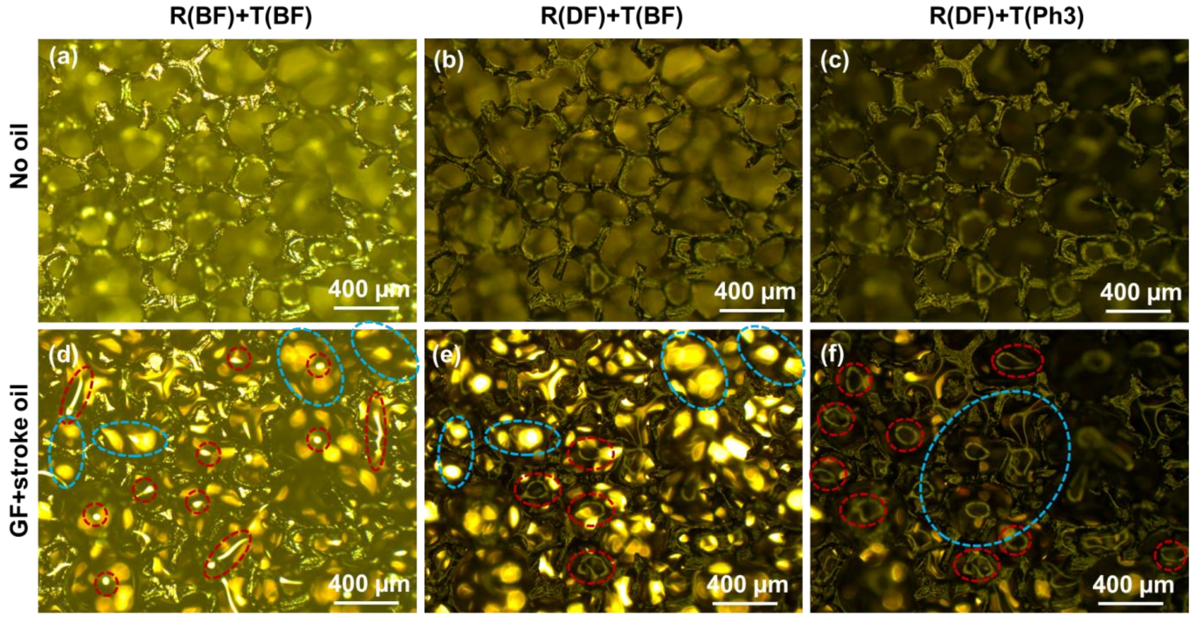

Figure 3. Optical images of graphene foam (a)-(c) without and (d)-(f) with stroke oil. Images in each column are under the same detection mode, with (a), (d) under bright field (BF) reflected (R) and transmitted (T) light; (b), (e) under

dark field (DF) reflected and bright field transmitted light; (c),(f) under dark field reflected light and phase contrast (Ph3) transmitted light. In (d-f), oil appears as bright regions due to focusing effects. In DF mode the boundries of the oil droplets are clearly observed (marked by red circles). All of the images were taken on the same position. Images under other modes can be found in S2-5.

In Fig. 3(d-f) the presence of oil droplets can be clearly seen in the form of bright spots within GF. The oil droplets lead to the local optical focusing of the transmitted light causing bright regions. The DF mode allowed the visualisation of the edges of oil droplets (Fig. 3(f)), marked with red circles. The clear difference between a graphene/air and graphene/oil composite is the presence of these additional oil boundaries (interfaces) which lead to the scattering of incident light rays,[19] as discussed in the later experiments as well. Thus in this method, the presence of oil environments can be detected by comparing images of GF with and without oils in various modes.

Moreover, the possibility of differentiating the oil species by optical images is investigated. First, graphene foam was soaked with three oils, including supercut oil, turbo oil and stroke oil, which are transparent with different colours (Figure 4 (a)). Then the samples were detected under transmitted light, with (b)-(d) in bright field mode and (e)-(g) phase contrast mode. Images in the same column are illustrating identical positions of the same sample. Interestingly, oil droplets were observed as small light distortions in bright field and arc-like halos in phase contrast mode. The sizes of the oil droplets are about 10 µm, thus it is expected that geometric scattering will happen when light pass through the samples.

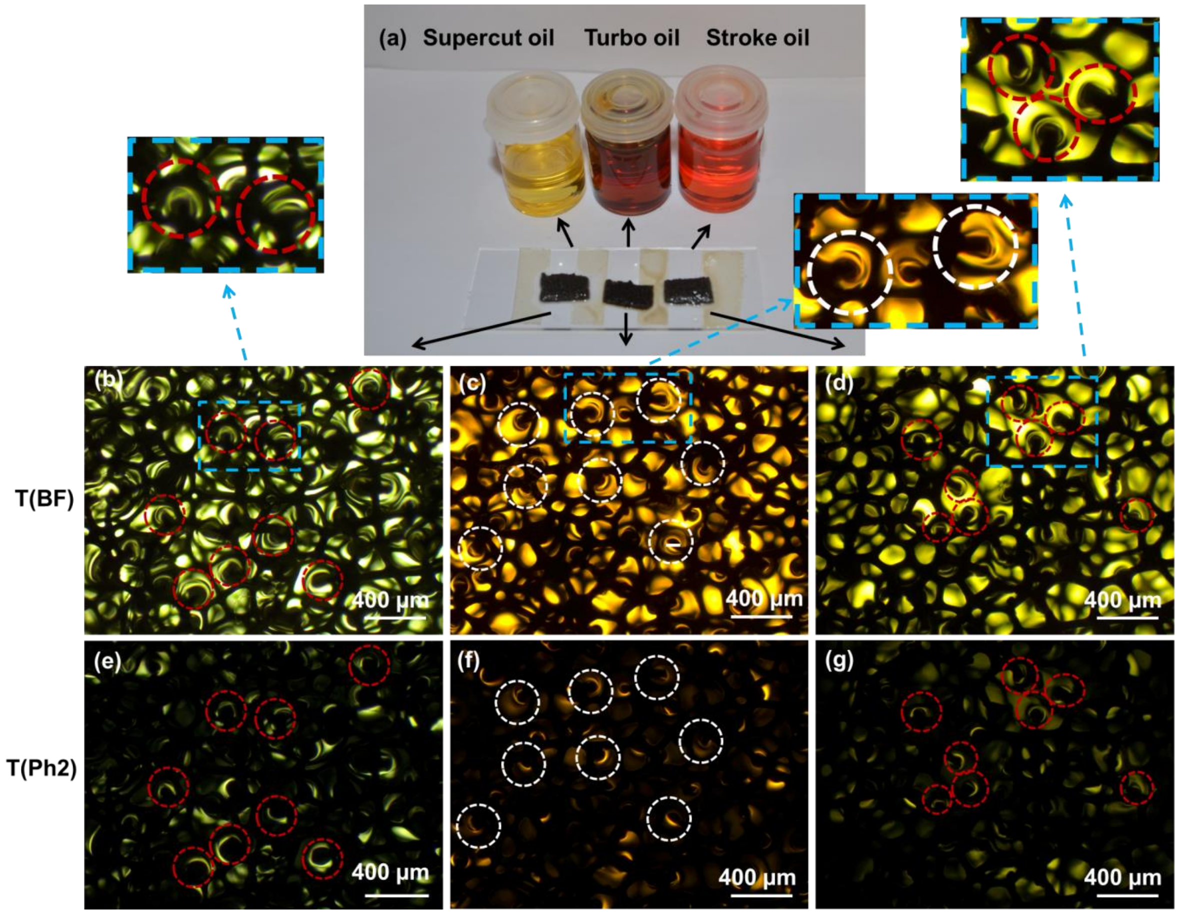

Figure 4. (a) Samples of different oils. Optical images of Graphene foam with (b) and (e) supercut oil, (c) and (f) turbo oil, (d) and (g) stroke oil. (b)-(d) are under bright field of transmitted light, while (e)-(g) are under phase contrast mode (Ph 2).

The difference colours of the oils in the bottles indicate different absorptions characteristic. As can be seen in Figure 4(a), supercut oil is bright yellow while stroke and turbo oil are reddish. Turbo oil has strongest absorption in shorter wavelengths range thus mostly the red light passes. The colours of the oils in the graphene foam differed from their original colour in the bottles; this may be due to the foam's absorption as well as the scattering effect. What can also be noticed is that the colours of supercut and stroke oils are very similar in the foam. However, more distortion can be seen when light pass though supercut oil as it is much thicker than the other two oils.

Images of crude oils in graphene foam are illustrated in Figure 5, in which the same row are for the same oil, with (a) Wattenberg field oil, (d) Spindletop field, (g) West Texas intermediate oil, and (j) Guffy field oil. The detection modes in each column was varied, with images in the first column taken under only bright field transmitted light (T(BF)), images in the second column with dark field reflected light (R(DF)), and images in the third column with both bright field transmitted light and dark field reflected light (T(BF)+R(DF)).

In transmitted light, different oil species in GF present distinct colour features. The crude oils (except for Guffy field oil) were mostly black coloured in the bottles and could not be differentiating by naked eyes, as demonstrated in S6. Guffy field oil in the bottle is extra light/transparent, similar to the specialised oils in Figure 4. Thus the appearance of Figure 5 (j), for Guffy field oil in GF is similar to images in Figure 4(b and d). As for the other three dark crude oils, the chemical and physical properties, associated with absorption and scattering effect respectively, would be different, which leads to the difference in images under transmitted light. The images for West Texas intermediate oil in Figure 5(g) are totally dark, indicating a very low transmittance of visible light, while the weak red colour of Wattenberg oil in image 5 (a) suggest only a small portion of red light passes (in agreement with Fig. 2d).

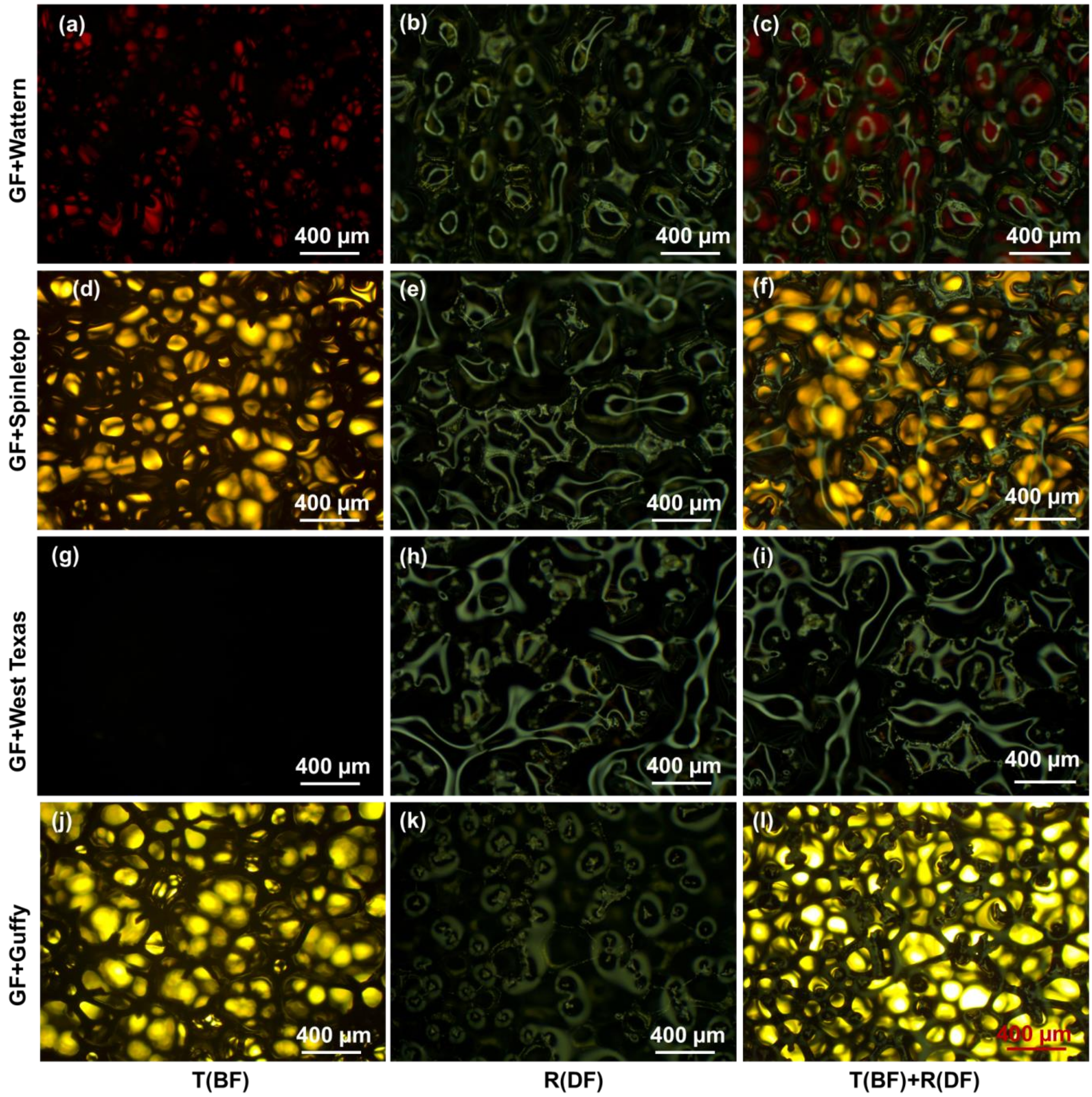

Figure 5. Optical images of graphene foam with crude oils. Each row of the images are with the same oil, with (a) Wattenberg field, (d) Spindletop field, (g) West Texas intermediate, and (j) Guffy field oil. Each column represents a different detection mode, with the first column for bright field transmitted light, second column for dark field reflected light, and the third column for both reflected (dark field) and transmitted (bright field) light.

The results for dark field reflected light are of interest as they present the oil distribution within the GF, even when the oil is highly absorbing and dark. The distribution of Wattenberg field oil (Figure 5(b)) is quite similar to Guffy field oil (5(k)), with oil forming smaller droplets, compared to the larger formless shapes presented by Spindletop field and West Texas oils (Fig. 5 e and (h)). The similar reflective optical images of oils in GF indicate similar surface oil distributions, which are associated with the oils physical properties, such as density, viscosity and temperature, etc. As for images in the third column, what can be seen is that they are superposition of images in the first and second columns. By combining the two optical modes, more physical and chemical properties of crude oils will be revealed. The images reveal the visible appearance of the GF/crude oil composite along with the oil droplet shapes and distribution. Optical images of crude oils taken under bright field reflected light are also shown in S7.

5.Graphene foam for oil spill sensing based on Light diffraction.

As discussed above, the oil droplets and their distribution in graphene foam may lead to light scattering. This is proven by the oil transmission spectra changes which occur when the oil species are soaked in GF (Figure 2). The imaging in various modes also suggests that oil droplets in GF cause optical focusing and their boundaries lead to optical scattering effects (Figure 4-5). To understand the effects of the presence of these droplets on the far filed transmission properties of GF, optical diffractions from GF (with and without oil) were studied. A customised angular diffraction set up was used with a red laser source of wavelength 650 nm. Figure 6(a) depicts the schematic of the diffraction measurement set up, while (b) shows a laser beam being transmitted through a GF sample. In the measurement setup, diffraction patterns were obtained by replacing the detector with a white screen and the patterns of the screen were captured by a camera. Then the screen was replaced by a detector to measure the angular optical intensity. A stepper motor was used to rotate the sample stage horizontally between -90 to 90 degrees, with 1 degree resolution.

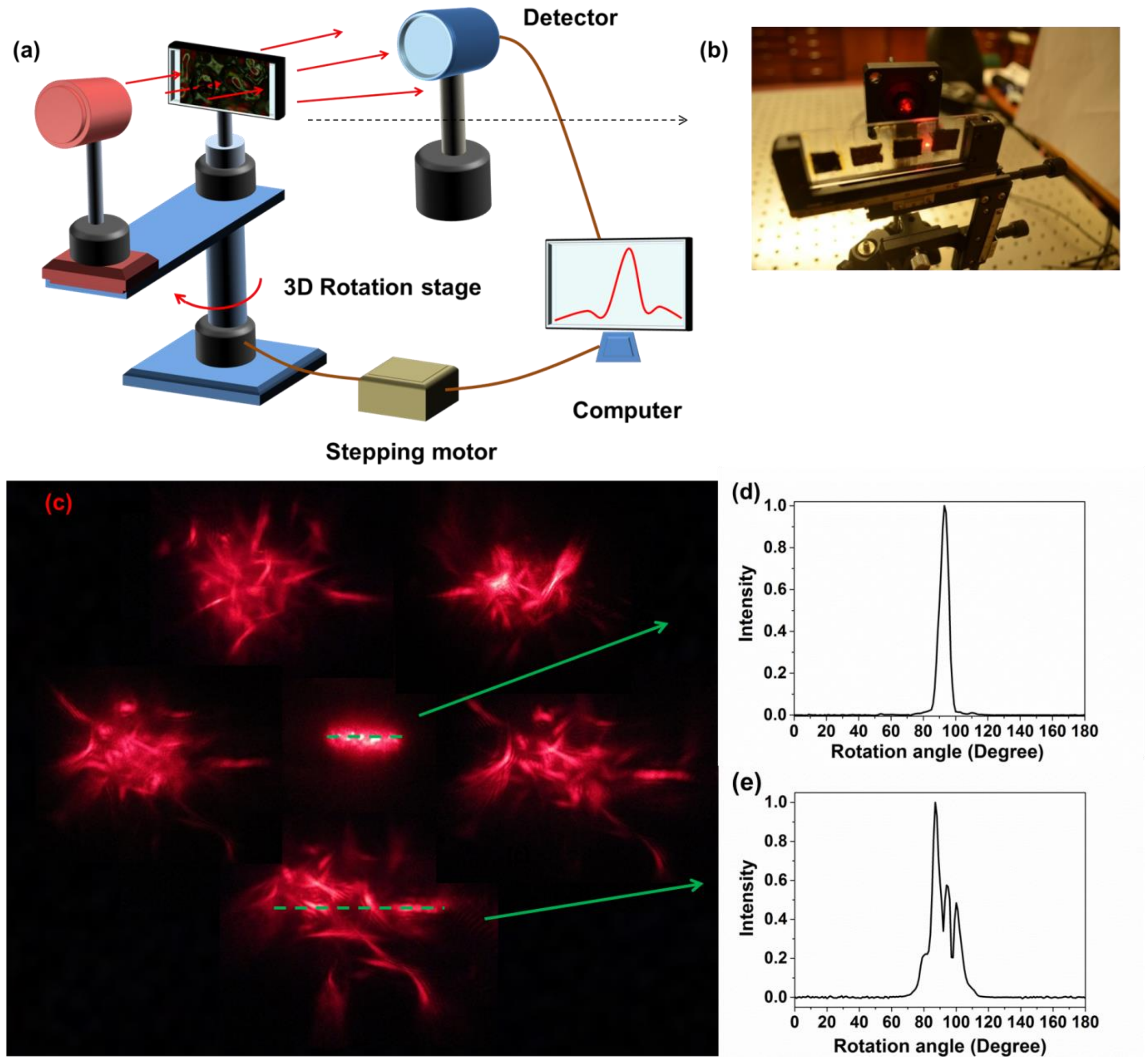

Figure 6. (a) and (b) Schematic and photo for the diffraction measurement set up. (c) Diffraction patterns when light transmitted through GF without oil (middle) and with stroke oil (sides). Different patterns can be obtained at various positions of the foam. Normalized light intensity along the green line across the pattern in the middle (d) and below (e).

Figure 6 (c) demonstrates diffractions of graphene foam with and without stroke oil. In the centre of Figure 6 (c), the pattern represents the light passing through graphene foam without any oil, and the shape is very similar to the pattern when light passing through glass slide, without any diffraction/scattering effects. However, when the light passes through graphene foam with stroke oil (phenomenon for stroke, turbo and supercut oils are similar) the diffraction pattern changes dramatically. The patterns generated from five different regions of the sample are shown in the corners of Figure 6(c). Figure 6(d and e) are illustrating the normalized light intensity along the green lines across the diffraction patterns in the middle and at the bottom, respectively. For graphene foam without oil, light intensity distribution has a sharp peak in the centre of the angular diffraction intensity pattern. The average pore size for graphene foam is in hundreds of microns (much larger than the wavelength of light), hence negligible diffraction/scattering of light occurs and a pronounce zero order peak (undiffracted light) is observed in the centre.

However, the light intensity gets distributed in the larger degree ranges when oil is added, as shown Figure 6(e). The three peaks in this figure are consistent with the three bright spots in the bottom pattern of Figure 6 (c). Optical scattering is a prominent effect that is displayed by the oil rich graphene foams. The focusing effects from each droplet and the scattering from the additional boundaries cause the spreading of the transmitted laser beams. This effect can be conveniently used for remote oil detection via optic fibres, where the presence of oil (after absorption in GF) will lead to sufficient drop in transmission efficiency. The scattered rays are less to be coupled and transported by the optic fibres to the detectors; hence a transmission drop will occur and likewise the spectral signature can be used for oil species recognition.

The diffractions of crude oils in graphene foam were also studied (Figure 7), Spindletop and Guffy oils shows distinguish diffraction effects. Because of the low transmission of Wattenberg and West Texas oil in graphene foam, no diffraction was observed. This can be explained by Figure 2 (d), in which no light passes through the West Texas oil in graphene foam while no more 10% light passes through the Wattenberg oil in the foam.

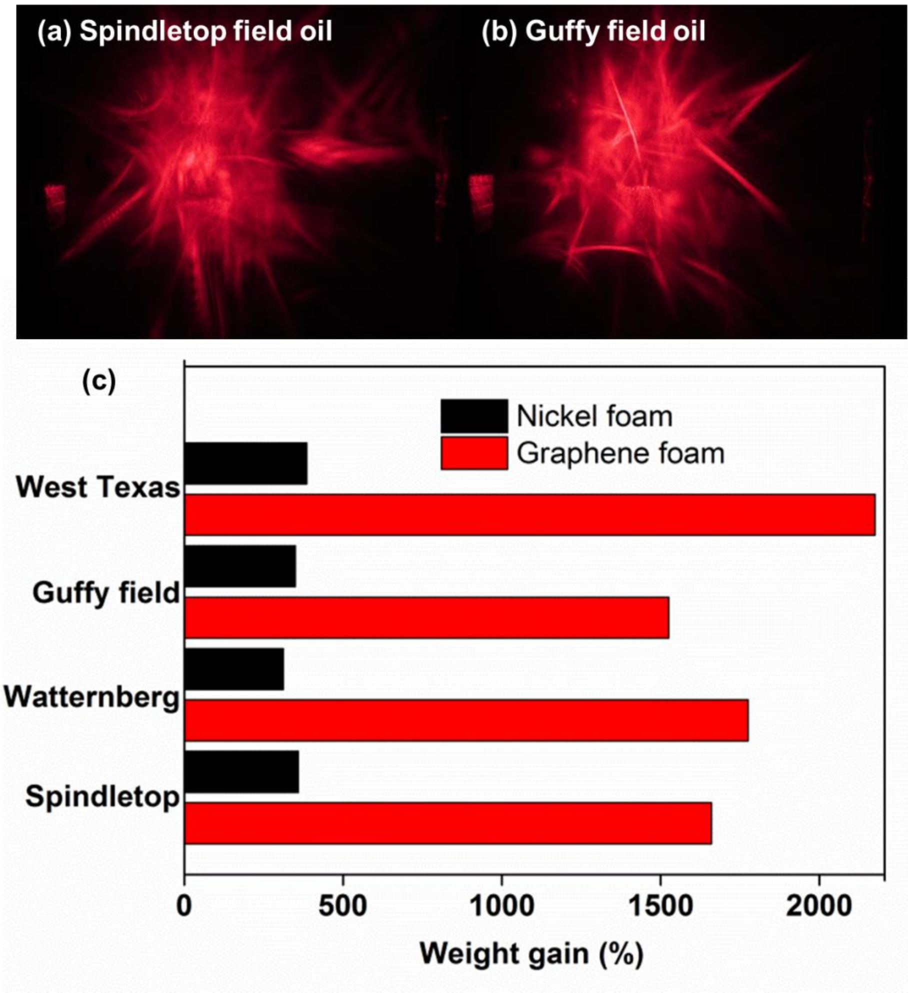

Figure 7. Diffraction patterns in response to incident red laser propagating through graphene foam soaked in (a) Spindletop field and (b) Guffy field crude

oils. (c) Absorption efficiencies of Graphene and Nickel foam. Graphene foam absorbs crude oils from West Texas (21.8×), Guffy field (15.3×), Wattenberg (17.8×), and Spindletop field (16.6×) with high efficiency compared with Nickel foam, with no more than 4 times weight gain.

To signify the superiority of graphene foam over a Ni based foam a comparison of absorption efficiencies (with crude oil samples) was performed (Figure 7(c)). For each of the oil sample, graphene foam has displayed higher efficiency than Nickel foam, which has weight gains of no more than 4 times for the oils. Due to the larger density, absorption efficiencies of both foams for West Texas oil are the highest, with near 21.8 times for graphene foam and 3.8 times for Nickel foam.

Conclusion

In conclusion, we proposed a simple and innovative way to detect oil environment by using graphene foam through optical imaging, as well as light scattering method. Compared with the existing methods, which detect oil emulsions or organism in the water and often involve complicate data processing, the graphene foam's performance as an oil collector can enhance the oil signal, making the detection easier, faster and economizer. Moreover, different oils in graphene foam give different colours in optical images, providing the possibility to identify the oil species. Interestingly, under microscope imaging, oil droplets can be observed in the graphene foam, which enhance the scattering effects, leading to the changes in spectral transmission. Despite the changes, the characteristic shapes of the transmission spectra remain the same, as well as the relative relationships between different oils. Finally diffraction of the oil in graphene foam was studied and results suggest that effect can be used to detect oil in conjunction with present optic fibre based oil sensors.

Corresponding Author

*h.butt@bham.ac.uk, Tel: +44 121 4158623, Fax: +44 121 414 3958

Present Addresses

†School of Mechanical Engineering, University of Birmingham, Edgbaston, Birmingham B15 2TT, UK

Author Contributions

The manuscript was written through contributions of all authors. All authors have given approval to the final version of the manuscript.

Acknowledgements

H. Butt would like to thank The Leverhulme Trust for the research funding.

References

[1] M. D. Long, "Remote Sensing for Offshore Marine Oil Spill Emergency Management, Security and Pollution Control.," 2012.

[2] B. M. I. (Battelle), "Capabilities and Uses of Sensor-Equipped Ocean Vehicles for Subsea and Surface Detection and Tracking of Oil Spills ", Report 2014.

[3] M. J. Hou, M. Kim, and D. O. Shah, "A light scattering study on the droplet size and interdroplet interaction in microemulsions of AOT—oil—water system," *Journal of Colloid and Interface Science,* vol. 123, pp. 398-412, 6// 1988.

[4] J. Rouch, A. Safouane, P. Tartaglia, and S. H. Chen, "Static and dynamic light scattering studies of water ‐ in ‐ oil microemulsions in the critical region. Evidence of a crossover effect," *The Journal of Chemical Physics,* vol. 90, pp. 3756-3764, 1989.

[5] D. M. Rubin, H. Chezar, J. N. Harney, D. J. Topping, T. S. Melis, and C. R. Sherwood, "Underwater microscope for measuring spatial and temporal changes in bed-sediment grain size," *Sedimentary Geology,* vol. 202, pp. 402-408, 12/1/ 2007.

[6] S. J. Kennelly and A. J. Underwood, "Underwater microscopic sampling of a sublittoral kelp community," *Journal of Experimental Marine Biology and Ecology,* vol. 76, pp. 67-78, 3/20/ 1984.

[7] T. Akiba and Y. Kakui, "Design and testing of an underwater microscope and image processing system for the study of zooplankton distribution," *Oceanic Engineering, IEEE Journal of,* vol. 25, pp. 97-104, 2000.

[8] E. B. Kujawinski, M. C. Kido Soule, D. L. Valentine, A. K. Boysen, K. Longnecker, and M. C. Redmond, "Fate of dispersants associated with the Deepwater Horizon oil spill," *Environmental science & technology,* vol. 45, pp. 1298-1306, 2011.

[9] M. J. Hemmer, M. G. Barron, and R. M. Greene, "Comparative toxicity of eight oil dispersants, Louisiana sweet crude oil (LSC), and chemically dispersed LSC to two aquatic test species," *Environmental Toxicology and Chemistry,* vol. 30, pp. 2244-2252, 2011.

[10] C. M. Couillard, K. Lee, B. Légaré, and T. L. King, "Effect of dispersant on the composition of the water ‐ accommodated fraction of crude oil and its toxicity to larval marine fish," *Environmental Toxicology and Chemistry,* vol. 24, pp. 1496-1504, 2005.

[11] T. C. Hazen, E. A. Dubinsky, T. Z. DeSantis, G. L. Andersen, Y. M. Piceno, N. Singh*, et al.*, "Deep-sea oil plume enriches indigenous oil-degrading bacteria," *Science,* vol. 330, pp. 204-208, 2010.

[12] F. Zhang, Y.-H. She, H.-M. Li, X.-T. Zhang, F.-C. Shu, Z.-L. Wang*, et al.*, "Impact of an indigenous microbial enhanced oil recovery field trial on microbial community structure in a high pour-point oil reservoir," *Applied microbiology and biotechnology,* vol. 95, pp. 811-821, 2012.

[13] X.-T. Kong, A. A. Khan, P. R. Kidambi, S. Deng, A. K. Yetisen, B. Dlubak*, et al.*, "Graphene-Based Ultrathin Flat Lenses," *ACS Photonics,* vol. 2, pp. 200-207, 2015/02/18 2015.

[14] H. Bi, X. Xie, K. Yin, Y. Zhou, S. Wan, L. He*, et al.*, "Spongy graphene as a highly efficient and recyclable sorbent for oils and organic solvents," *Advanced Functional Materials,* vol. 22, pp. 4421-4425, 2012.

[15] H. Bi, X. Xie, K. Yin, Y. Zhou, S. Wan, R. S. Ruoff*, et al.*, "Highly enhanced performance of spongy graphene as an oil sorbent," *Journal of Materials Chemistry A,* vol. 2, pp. 1652-1656, 2014.

[16] X. Huang, B. Sun, D. Su, D. Zhao, and G. Wang, "Soft-template synthesis of 3D porous graphene foams with tunable architectures for lithium–O 2 batteries and oil adsorption applications," *Journal of Materials Chemistry A,* vol. 2, pp. 7973-7979, 2014.

[17] D. N. Tran, S. Kabiri, T. R. Sim, and D. Losic, "Selective adsorption of oil–water mixtures using polydimethylsiloxane (PDMS)–graphene sponges," *Environmental Science: Water Research & Technology,* vol. 1, pp. 298-305, 2015.

[18] K. Xi, P. R. Kidambi, R. Chen, C. Gao, X. Peng, C. Ducati*, et al.*, "Binder free three-dimensional sulphur/few-layer graphene foam cathode with enhanced high-rate capability for rechargeable lithium sulphur batteries," *Nanoscale,* vol. 6, pp. 5746-5753, 2014.

[19] H. Butt, P. R. Kidambi, B. Dlubak, Y. Montelongo, A. Palani, G. A. J. Amaratunga*, et al.*, "Visible Diffraction from Graphene and Its Application in Holograms," *Advanced Optical Materials,* vol. 1, pp. 869-874, 2013.